Development of Spin Coated Mesoporous Oxide Films for MEMS Structures

JONG-AH PAIK,[1]* SHIH-KANG FAN,[2] HSIN CHANG,[3] CHANG-JIN KIM,[2]
MING C. WU,[3] & BRUCE DUNN [1]

[1]*Departments of Materials Science and Engineering*
[2]*Mechanical and Aerospace Engineering*
[3]*Electrical Engineering University of California, Los Angeles, CA 90095, USA*

Abstract. Mesoporous materials offer several unique properties when incorporated in microelectromechanical systems (MEMS) including low density, thermal insulation and the ability to carry out rapid etching. This paper describes the development of two mesoporous thin film materials for MEMS structures, an organically modified silicate and crystalline TiO_2. The morphologies of the mesoporous thin films are similar in that they have approximately 50% volume porosity, an average pore diameter of ~5 nm, and a narrow pore size distribution. However, the chemistries of the two materials are very different as are their properties for MEMS applications. The organically modified silicate film is designed to have controlled hydrophobicity. CH_3 groups which are present in the sol precursor are retained in the final material despite the 400°C calcination temperature used for producing the porous mesostructure. Contact angles as high as 80 degrees have been achieved. The mesoporous TiO_2 is designed to have resistance to HF etching. Heat treatments of the mesoporous material are carefully controlled enabling the TiO_2 pore walls to crystallize without collapsing the pore network structure. A combination of anatase and rutile phases are produced in the solid phase and exhibit excellent resistance to HF.

Keywords: mesoporous oxide films, spin coating, MEMS, surface micromachining

Introduction

Mesostructured materials have attracted worldwide interest since the discovery of M41S in 1992 [1]. Since that time mesoporous materials have been used in several applications including catalysis, filtration, and encapsulation. Mesoporous silica has been the most widely studied system and powders [1, 2], fibers [3] and thin films [4, 5] of mesoporous silica have been produced with varying pore sizes (2 to 50 nm) and organized structures (i.e., hexagonal, cubic, lamellar). Mesoporous metal oxides other than silica have also been reported, although this field has received much less attention as each composition requires that specific synthetic strategies be developed [6].

The present paper is directed at the development of mesoporous materials for microelectromechanical systems (MEMS) applications. MEMS are systems composed of microfabricated electronic and non-electronic elements which are designed to perform actuation, control, and acquisition and processing of signals [7]. MEMS technology has grown dramatically during the past decade and high volume commercial markets for MEMS devices have been established in a variety of areas including the automotive industry, ink-jet printing, optical systems and chemical/biological sensing [8]. The incorporation of new materials can enhance MEMS devices since the properties of materials are intimately related to the performance of MEMS devices. Our initial work in this area involved the incorporation of mesoporous silicon oxide and aluminum oxide into basic MEMS structures [9]. Mesoporous alumina was fabricated into microbridges, cantilevers

*To whom all correspondence should be addressed. E-mail: japaik@hotmail.com

(a) Micro bridges

(b) Cantilever
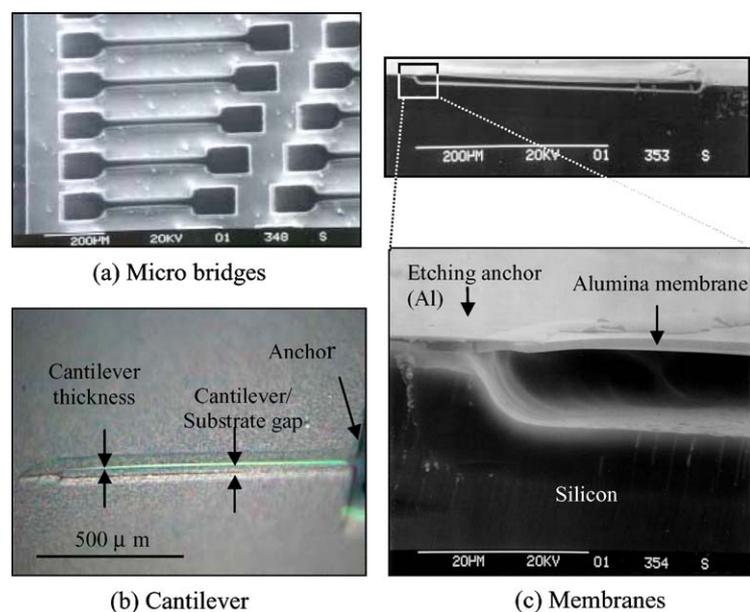
(c) Membranes

Fig. 1. Mesoporous alumina fabricated into micro bridges, cantilevers, and membranes (The structures were released by XeF$_2$ dry etching of the silicon substrate).

and membranes as shown in Fig. 1. These first studies demonstrated the ability to use mesoporous oxide films both as a sacrificial layer and as a structure layer. For example, mesoporous silica films are attractive for releasing large area structures because the etching rate in HF solutions is over 30 times faster than that of phosphosilicate glass (PSG), the commonly used sacrificial layer in the MUMPs (multiuser MEMS processes) process [10]. Mesoporous alumina shows different etching characteristics from that of mesoporous silica and has been used as a structure layer for applications requiring low density. We are currently exploring the use of mesoporous films for on-chip packaging applications, where the intrinsic porosity enables the wet etchant to penetrate the oxide film and remove the underlying sacrificial layer.

In this paper we extend our work on mesoporous materials to include organically modified systems and materials in which the oxide walls have crystallized. The former leads to materials with tunable hydrophobic character while the latter exploits the ability of crystalline TiO$_2$ to resist HF etching.

Experimental

Mesoporous films were prepared by modifying sol-gel methods to incorporate the block copolymer template.

The methods for synthesizing mesoporous SiO$_2$ and aluminum oxide were reported previously [9]. In the current investigation, the organically modified material was prepared using a similar methodology, as two precursors were used: tetraethyl orthosilicate (TEOS) and methyltriethoxy silane (MTES). The structure-directing agent was a commercially available, amphiphilic, triblock copolymer of the type poly (ethylene oxide)-*block*-poly (propylene oxide)-*block*-poly (ethylene oxide)-*block* (PEO-PPO-PEO) which is known to form ordered mesostructures [11]. Components of each coating solution are listed in Table 1. Once the coating solution was prepared, films were spin coated on silicon wafers at 2500 rpm for 1 minute, followed by drying at 100°C. The films were then calcined at ~400°C to produce the porous mesostructure.

The mesoporous titanium dioxide was prepared from a coating solution containing a block copolymer and a titania precursor, titanium butoxide. Spin coated films were heat treated at 100°C followed by a higher temperature treatment at 600°C. At this temperature, not only does the surfactant volatilize but the matrix crystallizes. A range of heat treatment temperatures between 100°C and 700°C were investigated and showed how the crystal morphology and phase changed as a function of heat treatment temperature. The constituents for each coating solution are listed in Table 1.

Table 1. Components of coating solutions and processing conditions for mesoporous films.

	Precursor	Solvent	Acid	Surfactant	Processing
Silica [13]	TEOS (tetraethyl orthosilicate)	ethanol + water	HCl	Pluronic F127 ($EO_{106}PO_{70}EO_{106}$)	aging : 100°C burn out: 400°C 5000 Å/layer
Alumina [14]	ASB (aluminum-sec-butoxide)	ethanol + water	HNO_3	Pluronic F127 ($EO_{106}PO_{70}EO_{106}$)	aging: 100°C burn out: 500°C 3000 Å/layer
Hybrid silica	TEOS + MTES (methyltriethoxysilane)	ethanol + water	HCl	Pluronic F127 ($EO_{106}PO_{70}EO_{106}$)	aging: 100°C burn out: 400°C 6000 Å/layer
Titania	TBT (titanium butoxide)	butanol + water	HNO_3	Pluronic 65 ($EO_{19}PO_{30}EO_{19}$)	aging: 100°C burn out: 600°C 2500 Å / layer

The physical and chemical properties of the mesoporous films were determined by various methods as described previously [9]. X-ray diffraction was used to determine the presence of ordered phases in the films, while transmission electron microscopy provided visual evidence of pore size, pore size distribution and the presence of mesoscopic order. Fourier transform infrared (FTIR) measurements and thermogravimetric analysis provided insight concerning the chemical changes that occurred during heat treatment. Surface roughness of the final films was determined by interferometry and atomic force microscopy, and ellipsometry was used as a rapid, non-destructive technique for determining film porosity. By combining these characterization methods, we were able to establish the interrelationship between solution composition, porosity and the presence of mesoscopic order in the films. For the organically modified mesoporous materials, contact angle measurements were carried out. In addition to measurements on films, we also characterized the morphology of mesoporous powders. The larger samples sizes available with powders enabled us to use gas adsorption analysis and, in this way, to compare films and powders of the same composition and processing method.

Results and Discussion

Figure 2 shows transmission electron microscopy (TEM) images for the various mesoporous films. These images clearly establish that the mesoporous oxide films are highly porous, the pores are interconnected and the pore diameter is quite uniform. The average

(a) Silica film   (b) Alumina film   (c) Hybrid film   (d) Titania film
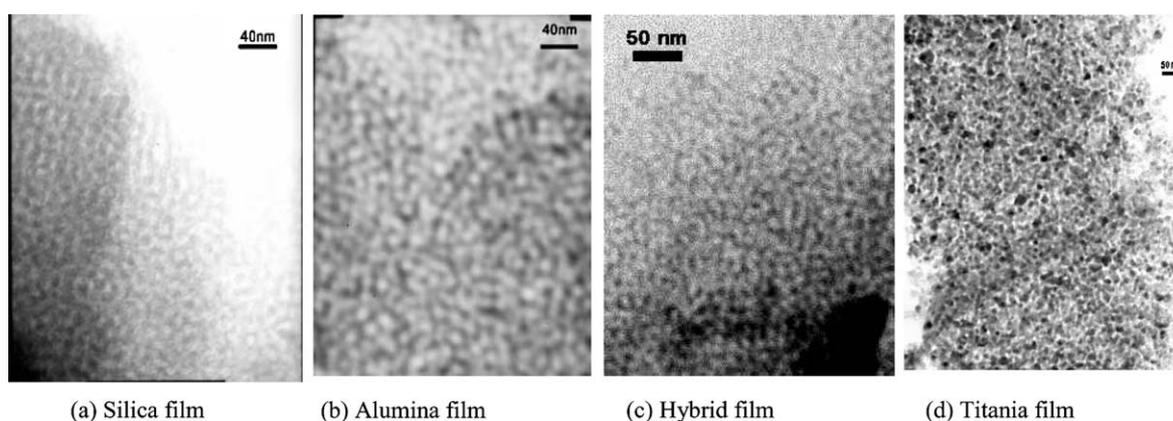
Fig. 2. TEM images for mesoporous films.

Table 2. Comparison between film properties and powder properties.

	Film properties		Powder properties	
	Approximate Pore Diameter ($\pm$1.5 nm) (from TEM image)	Porosity (vol%) ($\pm$3%) (from ellipsometry measurement)	Ave. pore diameter	Porosity (vol%) ($\pm$3 %)
Silica	8 nm	51	7 nm $\pm$ 2 nm	72
Alumina	8 nm	64	6 nm $\pm$ 2 nm	70
Hybrid silica	5 nm	49	4 nm $\pm$ 2 nm	43
Titania	5 nm	45	4 nm $\pm$ 1.5 nm	30

pore diameter for silica and alumina films is on the order of 8 nm, while that of the hybrid and titania films is a bit smaller at 5 nm. The pores are not ordered, however, by changing the specific composition of the solution, ordered porosity can be achieved [12]. For MEMS applications, we prefer that the porosity be disordered to ensure that through-hole etching processes are uniform.

Table 2 compares the porosity and pore diameter for both thin films and powders of the various mesoporous oxides. In general, the properties of the powders, where measurements are made using gas adsorption, are in reasonable agreement with the properties of the films, where measurements are based on TEM and ellipsometry. The one exception is titania, where the films are considerably more porous than the powders.

One property which we developed in the present study is that of mesoporous films with hydrophobic surfaces. We showed previously that heat-treated mesoporous films are extremely smooth [9], however we did not investigate their wetting properties. The current results demonstrate that altering the composition of the solid phase is able to control the wetting properties of the mesoporous film. Figure 3 shows that mesoporous silica films are hydrophilic. By synthesizing an organic/inorganic hybrid material, however, this property changes substantially. As the amount of methyltriethoxysilane (MTES) in the precursor solution is increased to a 1:1 molar ratio between MTES and tetraethylorthosilicate (TEOS), the contact angle increased from less than 10 degrees to approximately 80 degrees. Although not shown here, FTIR spectra indicate the presence of CH_3 groups from MTES in the final mesoporous films. That is, the calcination temperature of 400°C was sufficient to volatilize the surfactant and produce mesoporosity, but the CH_3 groups are retained in the films as evidenced by Si-CH_3 vibrations at 836 cm^{-1} and 1273 cm^{-1}. In addition, chemical analysis indicates that approximately 70% of the initially added CH_3 groups survive the heat treatment required to produce the mesoporous nanostructure. The surface micromachining methods reported previously [9] are readily extended to the mesoporous hybrid material. In particular, we have emphasized the use of dry etching with XeF$_2$ to fabricate membrane structures (similar

TEOS only
contact angle : <10 °

TEOS : MTES = 2:1
contact angle : ~ 40 °

TEOS : MTES = 1:1
contact angle : ~ 80 °
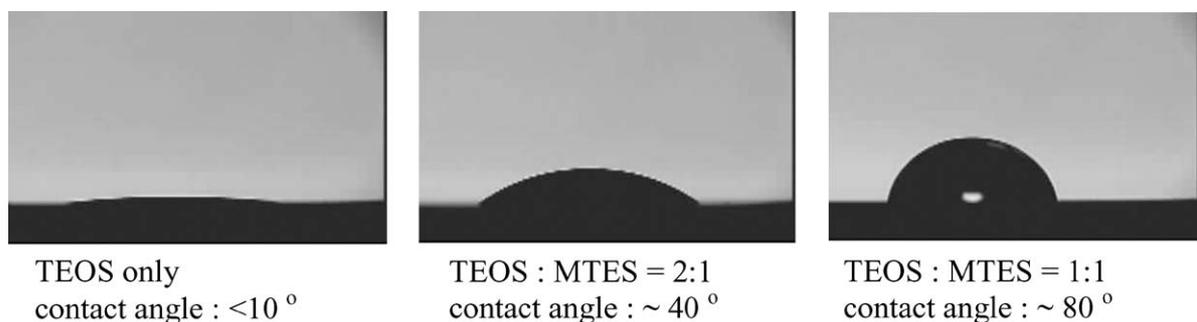
Fig. 3. Contact angle measurement of several silica mesoporous films with different molar ratio between TEOS and MTES as precursor.

to that of Fig. 1(c)) with the organic/inorganic hybrid materials.

The interest in fabricating mesoporous TiO_2 films arises from the fact that crystalline forms of TiO_2, particularly the rutile phase, are resistant to attack by HF solutions. Thus, a mesoporous TiO_2 film is capable of serving as a structure layer in which a sacrificial layer of PSG can be etched by having HF penetrate the mesoporous structure. A vital feature here is that the TiO_2 must be crystalline to exhibit the chemical resistance, but that the crystallization process must not cause the mesoporous structure to collapse. We have accomplished this by carefully controlling the crystallization process. As shown in Fig. 4, heat treatment of TiO_2 causes the formation of anatase at temperatures above $400°C$ and that rutile appears at $700°C$. The breadth of the X-ray diffraction peaks indicates that these crystallites are on the order of a few nanometers, comparable to the width of the pore walls. At temperatures above $800°C$, the mesoporous structure collapses and we no longer have the fine network of mesoscale pores as shown in Fig. 2(d).

Mesoporous, nanocrystalline TiO_2 films demonstrate considerable resistance to HF etching. In these experiments, a 250 nm TiO_2 film was deposited on a sapphire wafer (which is inert to HF), heat treated at $600°C$ and exposed to various etching solutions for 30 minutes. The standard solution used in these studies is a commercial buffered oxide etchant (BOE) solution which is commonly used for etching PSG and other silicate glasses. Commercial BOE contains 7%

Fig. 5. Etching test results of mesoporous TiO_2 films in buffered HF solution.

HF and, as shown in Fig. 5, mesoporous TiO_2 films exhibit no apparent etching at this concentration of HF. Only when the HF concentration was raised to $\sim28\%$ HF (4 times the commercial amount) were films slowly etched. These results with TiO_2 are the first ones to demonstrate mesoporous oxide films with HF resistance.

Conclusions

This paper extends our previous work in which we incorporated mesoporous oxide films in MEMS structures. In the present study, we developed two different types of mesoporous thin film materials and have begun to integrate them in MEMS processes. One material is an organic/inorganic hybrid material which exhibits hydrophobic behavior. The ability to tailor the hydrophobicity of surfaces is important in MEMS technology because the high surface-to-volume ratio in small devices strongly influences the transport of fluids. The mesoporous nature of this material enables gases to penetrate the structure, but not aqueous solutions. The second material presented is mesoporous TiO_2 which has been carefully crystallized so that the material exhibits good etch resistance to HF solutions. This is the first report of a mesoporous oxide that withstands HF etching, enabling it to have considerable promise as a porous structure layer in device applications. In addition to these specific properties, the two materials also exhibit the characteristic properties of mesoporous

Fig. 4. X-ray diffraction patterns of TiO_2 powders with different heating temperature.

oxide films presented in our initial work. The thin films are highly porous, with pore diameters <8 nm and a very narrow pore size distribution (±2 nm). The surface of these mesoporous films is extremely smooth (5 nm range) and metal layers deposited on mesoporous surfaces remain intact and are unaffected by the porous microstructure.

Acknowledgment

References

1. C.T. Kresge, M.E. Leonowicz, W.J. Roth, J.C. Vartuli, and J.S. Beck, *Nature*, **359**, 710 (1992).
2. P. Yang, D. Zhao, D.I. Margolese, B.F. Chmelka, and G.D. Stucky, *Chem. Mater.*, **11**, 2813 (1999).
3. H. Yang, G.A. Ozin, and C.T. Kresge, *Adv. Mater.*, **10**, 883 (1998).
4. D. Zhao, P. Yang, N. Melosh, J. Feng, B.F. Chmelka, and G.D. Stucky, *Adv. Mater.*, **10**, 1380 (1998).
5. Y. Lu, R. Ganguli, E.A. Drewien, M.T. Anderson, C. J. Brinker, W. Gong, Y. Guo, H. Soyez, B. Dunn, M.H. Huang, and J.I. Zink, *Nature*, **389**, 364 (1997).
6. F. Schuth, *Chem. Mater.*, **13**, 3184 (2001).
7. S.D. Senturia, *Microsystem Design* (Kluwer Academic Publishers, Boston, 2001).
8. See special issue of MRS Bulletin, April, 2001, *Microelectromechanical Systems: Technology and Applications*, D. Bishop, A. Heuer and D. Williams guest editors, p. 282.
9. J-A. Paik, S-K. Fan, C-J. Kim, M. C. Wu, and B. Dunn, *J. Mater. Res.*, **17**, 2121 (2002).
10. K.R. Williams and R.S. Muller, *J. Microelectromechan. Syst.*, **5**, 256 (1996).
11. B. Chu and Z. Zhou, in *Nonionic Surfactants: Polyoxyalkylene Block Copolymers*, edited by V.M. Nace (Marcel Dekker Inc., New York, 1996), p. 67.
12. J-A. Paik and B. Dunn, to be submitted.
13. D. Zhao, Q. Huo, J. Feng, B.F. Chmelka, and G.D. Stucky, *J. Am. Chem. Soc.*, **120**, 6024 (1998).
14. D.J. Suh and T.-J. Park, *Chem. Mater.*, **9**, 1903 (1997).